An *in situ* study of the effect of tin on the passivation of lead–tin alloys

P. Simon, N. Bui and F. Dabosi

Ecole Nationale Supérieure de Chimie de Toulouse, Laboratoire de Métallurgie Physique, URA 445, 118 route de Narbonne, 31077 Toulouse (France)

(Received September 2, 1993; in revised form December 10, 1993; accepted December 11, 1993).

Abstract

In lead/acid batteries, positive grids made of pure lead or low-antimony lead alloy have the disadvantage of developing a passive layer which impedes the electronic conduction through the electrode. The addition of tin to lead alloys has proved to overcome this passivation phenomenon and to increase the charge and discharge capacity of the lead batteries. In this work, lead–tin alloys were prepared with increasing tin levels up to 2.5 wt.%. These alloys were first passivated in a de-aerated solution of sodium tetraborate (pH = 9.1). Electronic conduction through this passive layer was evaluated by measuring the polarization currents of the ferro/ferricyanide couple which was added to the solution (pH = 9.1) in the passive potential range of the alloy electrode. The modification of the electronic conductivity of the passive layer by alloying with tin led to a change in the kinetics of the redox-couple reaction. From the kinetic parameters, it was found that no electron transfer was observed on passive lead alloyed with less than 0.8 wt.% tin. Electronic conductivity of the passive layer, evaluated by the exchange-current density of the redox system, increased sharply when the alloying tin level increased from 0.8 to 1.5 wt.%; it reached a plateau at higher tin levels. The instability of the passive layer, as evaluated by the passive current density, varied inversely with the electronic conductivity.

Introduction

In the lead/acid batteries industry, lead alloys with a high antimony content (6–12 wt.%) have been extensively used in the manufacture of grids [1]. Among other advantages, alloying with antimony increases the resistance to passivation of the grids. However, the main disadvantage of the addition of antimony is the decrease in the hydrogen-evolution overpotential which results in loss of water from the electrolyte. With the modern tendency for industry to produce maintenance-free and valve-regulated batteries, loss of water is minimized by the use of low-antimony or antimony-free alloys. Other problems associated with these new alloys then appear: loss of cycling capacity; low performance of positive electrode, and low charge acceptance for deep-discharged batteries [2]. These disadvantages may be the result of the presence of a passive layer at the grid/active material interface. The nature of this layer has been identified as tetragonal PbO (noted as tet-PbO) developed under the lead sulfate layer [3–6] during the charge and discharge of the battery. Pavlov [7] and Ruestchi [8] have proposed a mechanism of the formation of tet-PbO. The most interesting point is the increase in pH to a value of 9.3 at the positive grid/lead sulfate interface. This alkalinity

0378-7753/94/$07.00 © 1994 Elsevier Sequoia. All rights reserved
SSDI 0378-7753(93)01893-M

favours the formation of tet-PbO and basic sulfate $PbO \cdot PbSO_4$. This passive layer is probably responsible for the low electronic conductivity of the positive electrode because of its semiconducting properties [9]. The semiconducting property may explain the decrease in charge acceptance and in charge and discharge capacity of the battery. To alleviate the problem of passivation of the grids, the addition of tin to lead has shown to be a good solution. Culpin *et al.* [10] and Nelson and Wisdom [11] recently made a comprehensive review of the literature on the 'tin effect'. The general finding is that tin has the properties of increasing the resistance to the passivation of the grids and of facilitating charge transfer through the grid/active-material interface. However, the influence of tin on intense long-term cycling use is not well known. Furthermore, the electronic properties of the PbO layer have not been studied by *in situ* measurements (by a direct method), and the mechanism of the action of tin on the properties of PbO has still to be elucidated. The question is how much tin has to be added to the lead to reach the optimal electrochemical properties. This work aims to contribute to the understanding of the effects of tin additions on the electrical conduction of the PbO layer. Experimental alloys were prepared by alloying pure lead (99.999 wt.%) with pure tin (99.99 wt.%) up to 2.5 wt.%. The formation of the passive layer on the alloys was controlled by electrochemical polarization in a solution of pH = 9.1. The electronic properties of the passive layer were evaluated by analysing the kinetics of redox reactions on the passive electrodes.

Experimental

Lead–tin alloys were prepared by melting weighed mixtures of pure lead (99.999 wt.%) and pure tin (99.99 wt.%) in alumina crucibles. Liquid alloys were homogenized by mechanical stirring and then solidified in alumina moulds surrounded by sand. Parts of these alloys were used to make working electrodes for electrochemical studies; the remaining parts served as metallographical and surface analysis samples. Control of the passive film growth capacity was achieved by the polarization technique, using Tacussel equipment composed of a potentiostat (PJT 100), a current recorder (EPC2) and an electronic millivoltmeter (ARIES 20000).

The electrochemical cell had a capacity of 250 cm^3. The auxiliary electrode was a 0.785 cm^2 platinum plate, the reference electrode was a mercury/mercurous sulfate electrode (SSE, +642 mV/NHE). All potentials reported in this study are versus SSE. Working electrodes were imbedded in cold mounting resin; their exposed surfaces were mechanically polished with emery paper under water, up to grade 1000; they were then washed in distilled water, and finally in absolute ethyl alcohol.

The electrolyte was 0.1 M $Na_2B_4O_7$ solution, de-aerated by purified argon. All the working electrodes were polarized at −2500 mV/SSE before each experiment in order to reduce the surface oxides formed during the mechanical polishing procedure. The redox couple was a solid mixture of potassium ferro- and ferricyanide salts of RP grade. When the passive film was grown completely by potential polarization, the mixture of the redox couple was added to the electrolyte in the cell at a concentration of 0.025 M for each form ($C_{Fe(II)} = C_{Fe(III)} = 0.025$ M). Then, the applied potential was scanned between 0 and −400 mV/SSE, in the passive domain of the electrodes.

The composition of the prepared alloys, already known by weighing of lead and tin elements before melting, was further checked by surface analysis, by X-ray energy dispersive spectroscopy (EDS). The measurements were carried out with a LINK eXL spectroscope (Oxford Instruments).

Results and discussion

Analysis and metallography of experimental alloys

The lead–tin phase diagram [12] shows that, at room temperature, the solid solubility of tin in lead is 1.9 wt.% in equilibrium conditions. To detect possible micro-segregation of tin in the experimental alloys, which were solidified in non-equilibrium conditions, energy dispersive spectroscopy (EDS) and metallography were used. Table 1 lists the EDS analysis results. The quantitative measurements by EDS gave values very close to those calculated by weight. EDS had an accuracy of 0.1 wt.% for tin.

Another technique of micro-segregation detection is metallography. Samples were etched with a reagent specially devised for this study [13]. The reagent gave rise to both chemical polishing and etching of the samples, which were previously mechanically ground under water with 1000 grit emery paper. Observations of etched samples through an optical metallographic microscope did not show micro-segregation of tin, even at grain boundaries. The microstructures of the alloys are shown in Figs. 1(a)–(g). Large grain sizes were observed because of the slow solidification of the alloys, exempt of impurities. In each grain, a particular mosaic structure was observed when etching was prolonged. For the Pb–2.5 wt.% Sn alloy, a dendritic structure was revealed. The interdendritic regions were richer in tin than the dendrites, but no particular segregation of tin, in precipitate form, was observed.

Electrochemical polarization of lead–tin alloys

Alloys were polarized in de-aerated 0.1 M $Na_2B_4O_7$ (pH = 9.1). Figure 2 shows the anodic polarization curve of pure lead, with a potential scan rate of 1 mV/s. The first anodic peak (A) appeared at −1030 mV and had a peak potential at −960 mV. It has been attributed to the formation of $Pb(OH)_2$ [14–17], lead borate $Pb_2B_4O_7$ or $Pb_2B_2O_4$ [18, 19]. In this study, X-ray photoelectron spectroscopy (XPS) surface analysis was used to identify the reaction taking place in this potential region. The working electrode was polarized up to −960 mV, maintained at this potential for 5 min, then removed from the cell, rinsed with distilled water, dried in a desiccator, then analysed by XPS (VG ESCALAB MKII). The element boron has not been detected in the surface film. One may assume that lead borate has not been formed during the first anodic reaction peak. Another experiment was carried out to verify that this peak formed in a basic solution did not contain any borate. A polarization experiment was then made in a solution of sodium hydroxide, pH varying between 9 and 9.5: a peak appeared at −1020 mV. This peak is probably related to the formation of lead

TABLE 1

Energy dispersive spectroscopy chemical analysis of Pb–Sn alloys

Alloy (wt.% Sn)	EDS analysis
0.5	0.5 (±0.1)
0.8	0.7 (±0.1)
1	1.0 (±0.1)
1.3	1.2 (±0.1)
1.5	1.5 (±0.1)
2.5	2.6 (±0.1)

hydroxide ($Pb(OH)_2$). The second peak (B) has been attributed to the formation of lead monoxide, PbO. From the US National Bureau of Standards' thermodynamic data [20], the equilibrium potential for $Pb(OH)_2/PbO$ is -891 mV at pH = 9.1. Figure 2 shows that peak (B) begins at -890 mV. XPS analysis made in this potential region confirmed the formation of PbO. After this peak, it is interesting to note the large region of passivity, between -650 mV and $+250$ mV, which occurred not only for pure lead, but also for the lead–tin alloys.

The existence of this passivity domain allowed the *in situ* study of electrical properties of the oxide film by using a redox couple with an equilibrium potential situated in this potential region. The ferri- and ferrocyanide couple is suitable, since its equilibrium potential in the $Na_2B_4O_7$ solution is -198 mV.

The third peak (C) has been identified as the oxidation of PbO in PbO_2 [18]. According to Pourbaix [21], the equilibrium potential of the PbO/PbO_2 system is

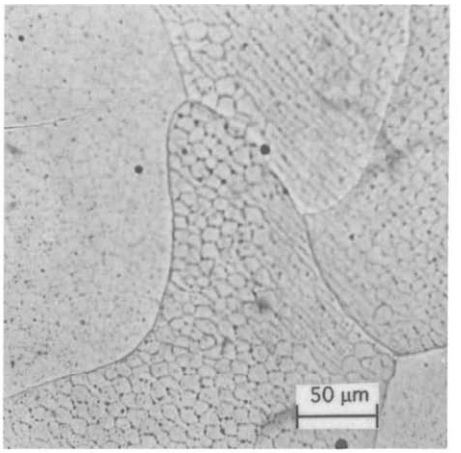

(a)

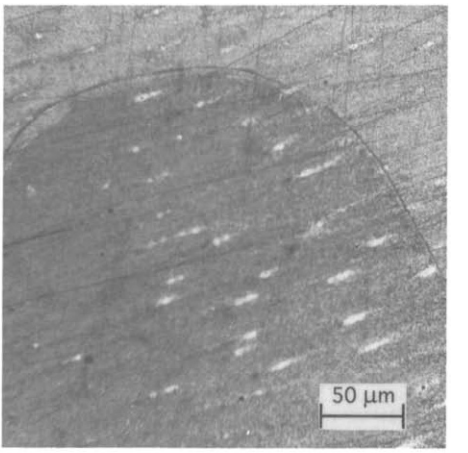

(b)

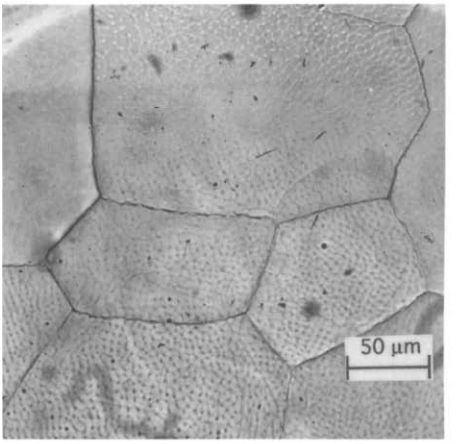

(c)

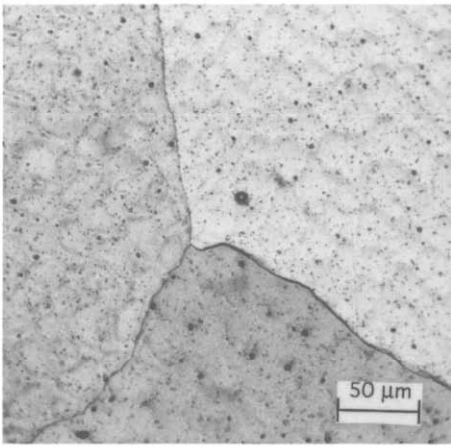

(d)

Fig. 1. *(continued)*

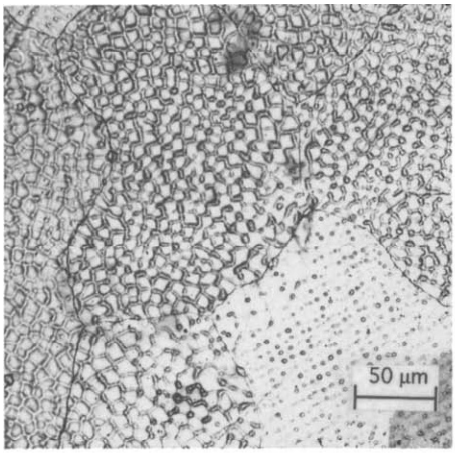

(e)

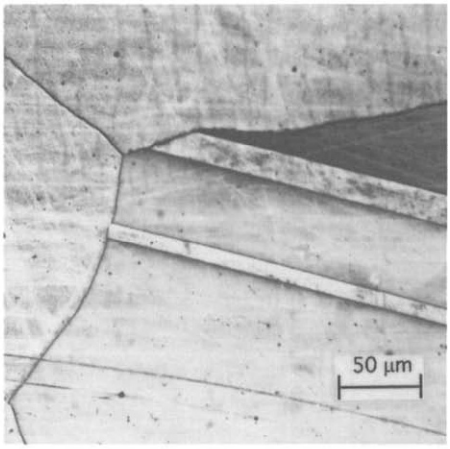

(f)

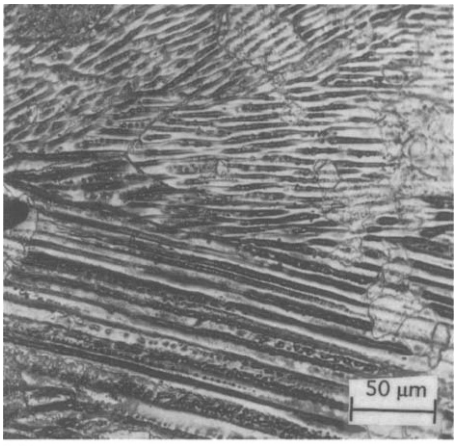

(g)

Fig. 1. (a) Micrography of cast lead; (b) micrography of Pb–0.5 wt.% Sn cast alloy; (c) micrography of Pb–0.8 wt.% Sn cast alloy; (d) micrography of Pb–1 wt.% Sn; (e) micrography of Pb–1.3 wt.% Sn cast alloy; (f) micrography of Pb–1.5 wt.% Sn cast alloy; (g) micrography of Pb–2.5 wt.% Sn cast alloy.

-100 mV, but the beginning of PbO_2 formation was observed at $+350$ mV (Fig. 2). This large overpotential was also observed in 1 M NaOH solution [14–17]. After the peak (C), the increase of current was due to the oxidation of water, with an oxygen evolution. The anodic polarization curves of the studied lead–tin alloys have the same shape as that of pure lead, but the most significant change lies in the values of the passive current density. It was observed that passive current density, at any potential, decreased as the polarization time increased. So, to evaluate the effect of alloying tin on the passive current density, each alloy was prepolarized for 5 min at -2500 mV, then polarized at 0 mV, that is in the middle of the passivity range, during a time long enough to attain a steady-state current. Figures 3 (a) and (b) show the change of the current density versus time, for the alloys polarized at 0 mV in the borate solution.

It can be seen that the steady-state passive current density (I_p) decreased when the tin content in lead alloys increased. This property is illustrated in Fig. 4.

Based upon the point of view of corrosion resistance, the value of the current density is usually related to the stability of the passive layer. The steady-state passive

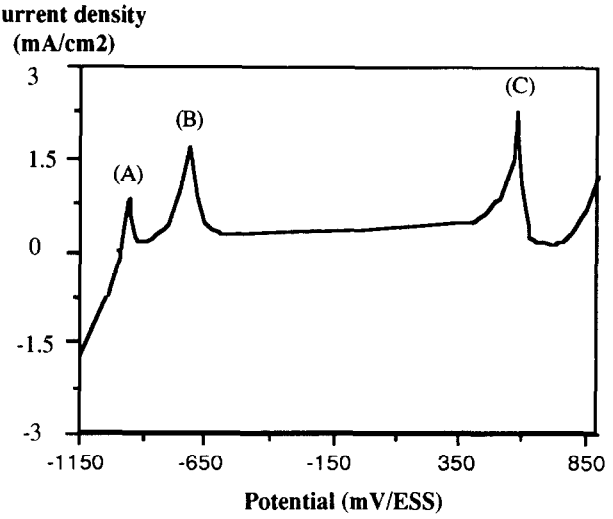

Fig. 2. Anodic polarization curve of pure lead in 0.1 M de-aerated $Na_2B_4O_7$ solution; scan rate: 1 mV/s.

current density, according to Vetter [22] represents the dissolution rate, which is equal to the formation rate of the passive layer. So, for a passive layer to be stable and protective, it must have a very low dissolution rate. For pure lead and lead–tin alloys, high I_p means high dissolution rate or high ionic activity of the oxide layer, in this case PbO. Above 1.5 wt.% Sn, I_p tends to be very low, $\sim 10^{-6}$ A/cm^2. In this work, the I_p of pure tin, as measured in the same conditions as lead–tin alloys, was 3.5×10^{-7} A/cm^2. So, the higher the tin content, the higher the corrosion resistance of the alloys in 0.1 M $Na_2B_4O_7$ solution. The change of I_p with the applied potential is shown in Fig. 5. Cyclic sweeping of potential between 0 and -400 mV was carried out by voltage steps of 10 mV, during a sufficient time to attain steady-state current values. It can be seen that I_p increased with potential only for low-tin alloys. It can be, therefore, concluded that the effect of tin is to increase the corrosion resistance and to increase the stability of the passivity versus the polarizing potential. This change of I_p with potential will be taken into account in the evaluation of the kinetics of the redox couple.

Polarization of the redox system

After the passivation of the working electrode by potentiostatic polarization between -400 and 0 mV, a mixture of potassium ferri- and ferrocyanide was added to the electrolyte (0.1 M $Na_2B_4O_7$) to reach a concentration of 0.025 M for each salt. When the redox system was fully dissolved, potentiostatic polarization was again scanned between -400 mV and 0 mV, and stationary currents were measured. The obtained polarization curves are given in Fig. 6. Even in the presence of the redox system, no additional current was observed for pure lead, 0.5 wt.% or 0.8 wt.% Sn alloys. This means that no transfer of electrons has taken place through the passive layer, preventing the oxidation of the ferrocyanide or the reduction of the ferricyanide. On the other hand, 1, 1.3, 1.5, and 2.5 wt.% lead–tin alloys allowed the redox reactions of ferri-/ferrocyanide to take place on their passive films. The currents measured were the sum of the passive currents of the alloys and the polarization currents of the redox

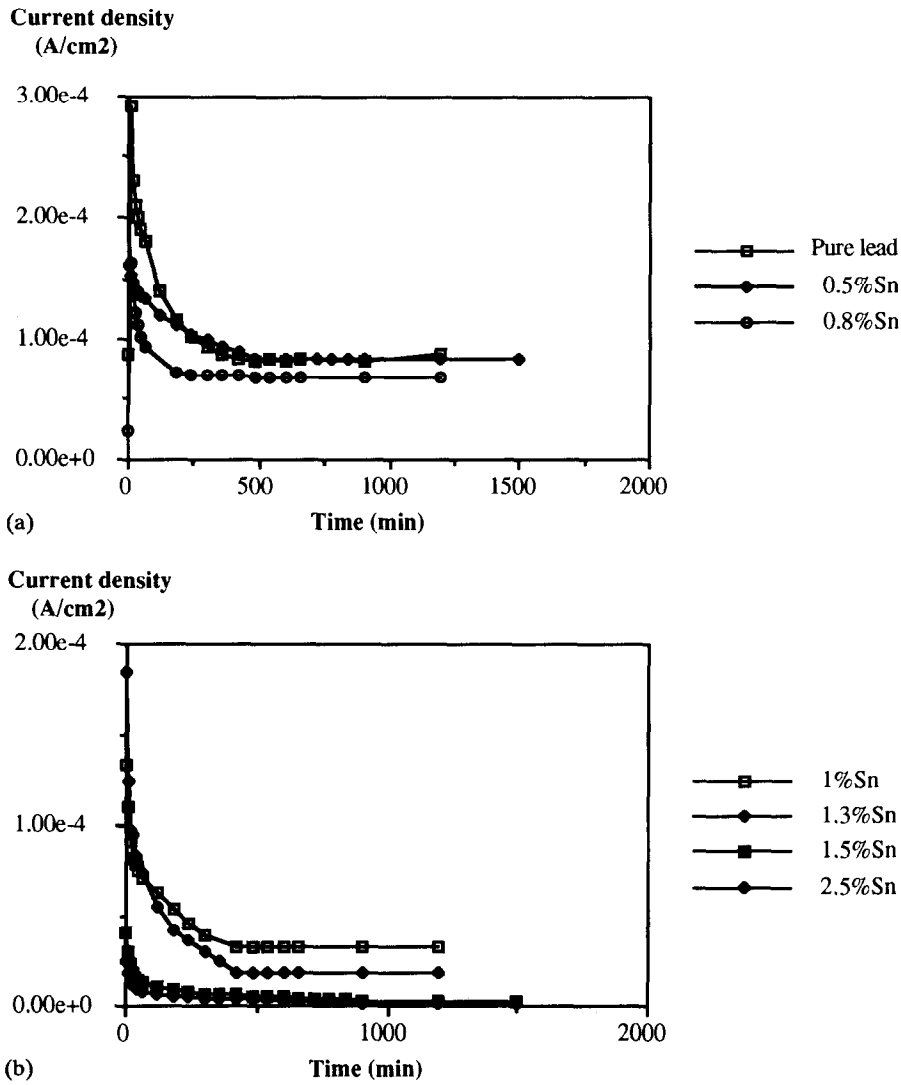

Fig. 3. (a) Current density vs. time plot for pure lead, 0.5 and 0.8 wt.% Sn lead–tin alloys during potentiostatic polarization at 0 V, in de-aerated 0.1 M $Na_2B_4O_7$ solution; (b) current density vs. time plot for 1, 1.3, 1,5, and 2.5 wt.% Sn lead–tin alloys during potentiostatic polarization at 0 V, in de-aerated 0.1 M $Na_2B_4O_7$ solution.

couple. The higher the alloying tin level, the higher the kinetics of the redox reaction. From this result, it can be stated that the passive films formed on alloys, having a tin content higher than 1%, present an electronic conductivity, while the low-tin alloy films present a rather ionic conductivity.

The total current densities in absolute values (Fig. 6) are considered to be $I_a = I_{a(redox)} + I_p$ and $I_c = I_{c(redox)} - I_p$. Polarization current densities of the redox reaction alone, $I_{a(redox)}$ and $I_{c(redox)}$, were calculated from these relations and are plotted in Fig. 7.

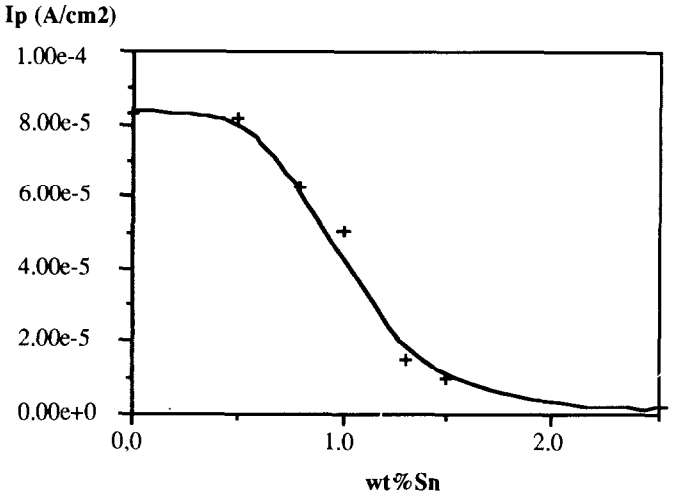

Fig. 4. Variations of the passivation currents (I_p) measured by potentiostatic polarization at 0 V, in de-aerated 0.1 M $Na_2B_4O_7$ solution.

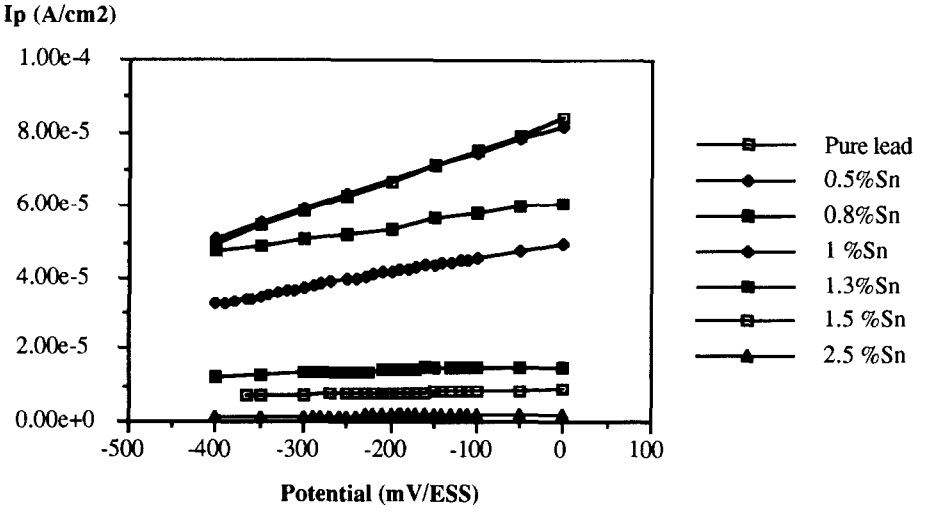

Fig. 5. Anodic polarization curves $I=f(V)$ between 0 and −400 mV for the different alloys studied, after polarization at 0 V, in de-aerated 0.1 M $Na_2B_4O_7$ solution.

It can be seen that the effect of alloying tin is to increase the redox-reaction rate, that is to facilitate electronic exchange at the alloy/solution interface. The tin content of the alloy must be higher than 1.5 wt.% to infer good electronic conductivity through the passive film. The redox kinetics decreased with lower tin contents, as can be seen for 1.3 and 1 wt.% alloys, then became negligible for 0.8, 0.5 wt.% and pure lead.

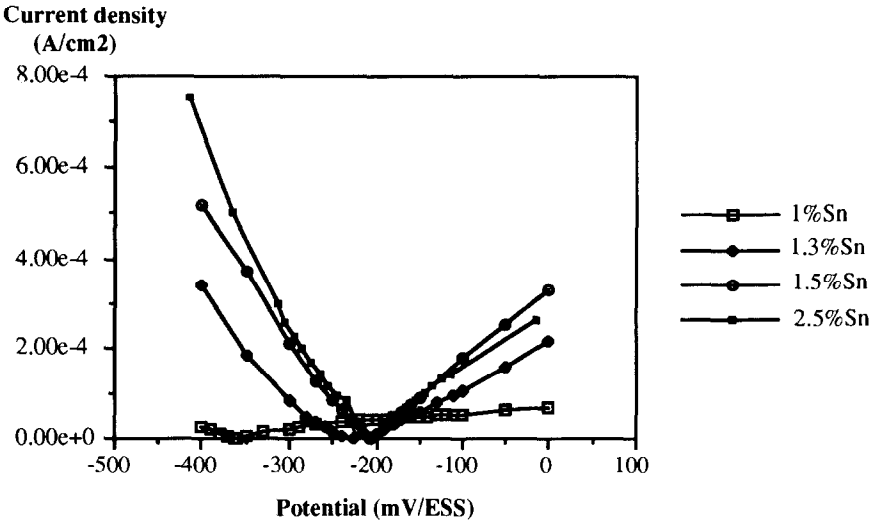

Fig. 6. Polarization curves of the studied alloys in de-aerated 0.1 M $Na_2B_4O_7$ solution containing 0.025 M ferri-/ferrocyanide.

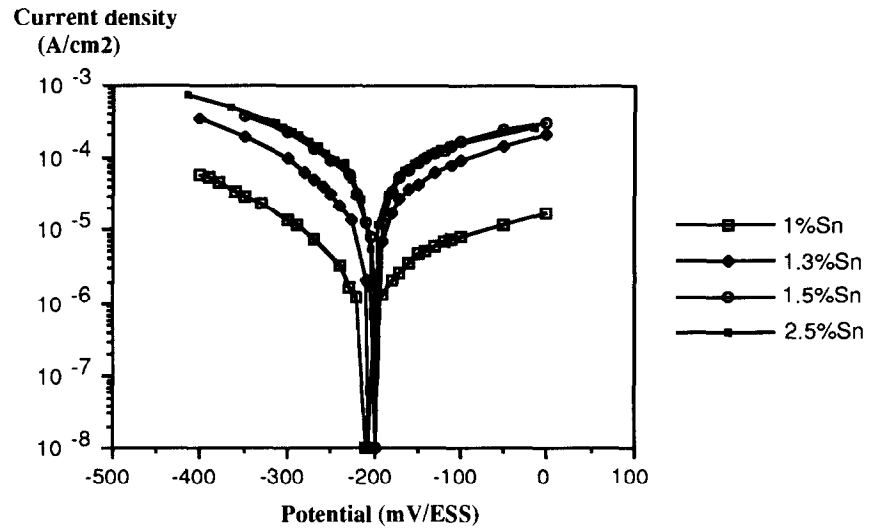

Fig. 7. Polarization curves of the ferri-/ferrocyanide couple (0.025 M) alone on lead–tin alloys in de-aerated 0.1 M $Na_2B_4O_7$ solution.

Kinetic parameters of the redox system

The values of the polarization currents and the applied potential for the redox reactions (Fig. 6) were used for calculation, by a 'Simplex' computing program [23, 24], of the anodic- and cathodic-transfer coefficients, the equilibrium potential and the exchange-current density. Usually, diffusion correction has to be carried out, but in this study, the passivity potential region is not large enough to attain the limiting current densities of the redox reactions. In order to minimize the error due to the

concentration polarization, only the low current values in a narrow range of potential around the equilibrium potential were taken into account in the computation: ±100 mV for low current densities (1 wt.% Sn alloys); ±80 mV for medium current densities (1.3 wt.% Sn alloy), and ±50 mV for high current densities (1.5 and 2.5 wt.% Sn alloys).

Since, around the equilibrium potential, the measured current is an algebraic sum of the anodic and cathodic currents, the relation $I_{app} = I_a + I_c$ was used in the calculation of I_a and I_c. In fact, the Butler–Volmer [25] eqn. (1) was the basis of the 'Simplex' computing program:

$$I = I_0 \times \{\exp[\alpha F/RT(E - E_{eq})] - \exp[-\beta F/RT(E - E_{eq})]\} \quad (1)$$

where the electron number n is 1, and the parameters α and β are the anodic and cathodic coefficients, respectively; I_0 is the exchange current density and E_{eq} is the equilibrium potential.

The calculated parameters were fitted to those of the Butler–Volmer eqn. with a correlation factor R_{corr} close to 100%. Tafel slopes b_a and b_c were calculated from eqns. (2) and (3):

$$b_a = RT/F\alpha \quad (2)$$

and,

$$b_c = RT/F\beta \ (n = 1) \quad (3)$$

From Table 2, it is interesting to note that the sum of the transfer coefficients, α and β, for each alloy, is much less than one unity. This property can be interpreted by the existence of a potential drop across the oxide film on the alloy surface. It is assumed that only a fraction of the applied potential was used to activate the redox reactions at the passive film/electrolyte interface. This interpretation has been proposed by Makrides [26] in his study of Fe^{2+}/Fe^{3+} reactions on passive electrodes (stainless steel, titanium, etc.). In this study, cathodic coefficient β and Tafel slope b_c have an almost constant value (Table 2), but the anodic coefficient α and Tafel slope b_a increase significantly with a varying tin content of the alloy. The increase in the values of α with increasing tin content can be related to the decrease in the potential drop across the passive layer. It is possible that the effect of tin, arised from the formation of SnO_2 – the only oxide stable in the studied potential and pH region – which increased the conductivity of the oxide layer, becomes an electronic conductor instead of an

TABLE 2

Computed kinetic parameters of the redox reaction obtained with the 'Simplex' method

Alloy	Tin content				
	1 wt.%	1.3 wt.%	1.5 wt.%	2.5 wt.%	100 wt.%
α	0.16	0.24	0.26	0.27	0.30
β	0.34	0.31	0.31	0.30	0.40
I_0 (A/cm^2)	4.66×10^{-6}	3.52×10^{-5}	7.83×10^{-5}	8.33×10^{-5}	1.28×10^{-4}
E_q (mV)	207	206	200	200	−195
R_{corr} (%)	99.97	99.92	99.87	99.99	99.91
b_a	0.358	0.242	0.219	0.211	0.20
b_c	0.172	0.189	0.187	0.199	0.144

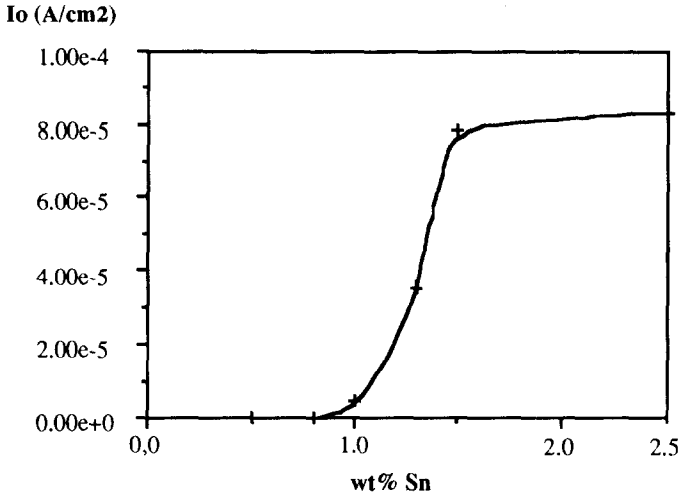

Fig. 8. Variation of the exchange-current density I_0 of the redox couple vs. tin content, in de-aerated 0.1 M $Na_2B_4O_7$ solution.

ionic conductor. The more the electronic conduction prevails, the smaller is the potential drop through the oxide film.

Figure 8 shows the change of exchange-current densities versus tin content in alloys. It can be seen that exchange-current density, I_0, is insignificant for alloys with less than 0.8 wt.% Sn. When the tin content increases from 1 to 1.5 wt.%, I_0 increases sharply, and attains a plateau from 1.5 to 2.5 wt.% Sn alloy. The change of I_0 illustrates the change of the conductivity of the film, from the ionic to the electronic type. The electronic conductivity of the passive film is assumed to be induced by the presence of SnO_2 resulting from the oxidation of the alloying tin. Surface analyses, mainly by XPS and EDS, are in progress to determine the amount of SnO_2 in the passive PbO film and to elucidate the mechanism of the role played by tin. The results will be reported in a future publication. Meanwhile, the first results obtained show that SnO_2 actually was present in the passive film.

Conclusions

In this *in situ* study of the effect of alloying tin on the conductivity of lead passive films, the following conclusions can be drawn:

1. The passive films of low-tin alloys (<0.8 wt.% Sn) have no electronic conductivity, but only ionic conductivity.

2. The electronic conductivity of the passive films increases sharply when the alloying tin content increases from 1 to 1.5 wt.% Sn, and attains a plateau between 1.5 and 2.5 wt.% Sn.

3. The passive current densities decrease or the corrosion resistance of lead–tin alloys increases, with an increasing tin content in the alloy.

4. The minimal tin content in lead–tin alloys, required to ensure a high electronic conductivity of the passive films (in pH=9) and a high resistance to corrosion, is ~ 1.5 wt.% Sn.

Acknowledgements

The authors are grateful to Mrs Michelle Reversat for her technical support and Mr Djar Oquab for the EDS chemical analyses.

References

1 D.M. Rice, *J. Power Sources, 28* (1989) 69–83.
2 R.T. Barton, P.J. Mitchell and F.A. Fleming, in T. Keily and B.W. Baxter (eds.), *Power Sources 13,* Research and Development in Non-Mechanical Electrical Power Sources, International Power Sources Committee, Leatherhead, UK, 1991, p. 25.
3 J. Burbank, *J. Electrochem. Soc., 103* (1956) 87.
4 J. Burbank, *J. Electrochem. Soc., 106* (1959) 369.
5 J. Lander, *J. Electrochem. Soc., 98* (1951) 213.
6 J. Lander, *J. Electrochem. Soc., 98* (1951) 220.
7 D. Pavlov, *Electrochim. Acta., 13* (1968) 205.
8 P. Ruestchi, *J. Electrochem. Soc., 98* (1973) 331.
9 A.N. Anastasievic, J. Garche and K. Wiesener, *J. Power Sources, 10* (1983) 43.
10 B. Culpin, D.A.J. Rand and A.F. Hollenkamp, *J. Power Sources, 38* (1992) 63–74.
11 R.F. Nelson and D.M. Wisdom, *J. Power Sources, 33* (1991) 165.
12 American Society for Metals (ed.), *Metals Handbook, Metallography, Structure and Phase Diagrams,* Vol. 8, 8th edn., 1973, p. 330.
13 M. Rerersat, P. Simon and N. Bui, *Rev. Metall. (Paris),* to be published.
14 M.T. Shevalier and V.I. Birss, *J. Electrochem. Soc., 134* (1987) 802.
15 M.T. Shevalier and V.I. Birss, *J. Electrochem. Soc., 134* (1987) 1594.
16 M.T. Shevalier and V.I. Birss, *J. Electrochem. Soc., 137* (1990) 2643.
17 V.I. Birss and W. Waudo, *Can. J. Chem., 67* (1989) 1098.
18 J.S. Buchanan, N.P. Freestone and L.M. Peter, *J. Electroanal. Chem., 182* (1985) 383.
19 A.A. Abdul Azim and M.M. Anwar, *Corros. Sci., 9* (1968) 245.
20 D.D. Wagman, W.H. Evans, V.B. Parker, I. Halow, S.M. Bailey and R.H. Schumm, *Tech. Note 270-3,* US National Bureau of Standards, 1968, p. 187.
21 M. Pourbaix, *Atlas of Electrochemical Equilibria in Aqueous Solutions,* 2nd edn., 1974, p. 485.
22 K.J. Vetter, *Z. Elektrochem., 62* (1958) 642.
23 J.A. Nelder and R. Mead, *Comput. J., 7* (1965) 308.
24 P.B. Ryan, R.L. Barr and H.D. Todd, *Anal. Chem., 52* (1980) 1460.
25 J.O'M. Bockris and A.K.N. Reddy, *Modern Electrochemistry,* Plenum, New York, 1970.
26 A.C. Makrides, *J. Electrochem. Soc., 111* (1964) 392.